Synthesis, characterization and photocatalytic activation of zinc nanoparticles via biogenic methods

ELİF ESRA ALTUNER
elifesraaltuner@gmail.com

Kocaeli Health and Technology University: Kocaeli Saglik ve Teknoloji Universitesi
https://orcid.org/0000-0001-7663-6898

Research Article

Keywords: Biogenic method, Dyestuff photodegradation, Photocatalytic studies, Zinc nanoparticles

Posted Date: April 29th, 2024

DOI: https://doi.org/10.21203/rs.3.rs-4021648/v1

Abstract

In this study, zinc nanoparticles (Zn NPs) were synthesized from the leaves of the plant *Hypericum calycinum* L by the biogenic method. Ultra-violet visible spectrum (UV-Vis), Fourier transmission electron spectroscopy (FTIR), transmission electron microscopy (TEM), and X-Ray were used to examine the absorbance, vibration bands, morphological structure, particle size, and crystalline size of the synthesized Zn NPs, respectively. Diffraction characterization (XRD) was performed. According to the results obtained, it was calculated that NPs gave peaks in the absorbance ranges of 274 and 370 nm, had a size of 29.066 ± 10.561 nm, and their crystalline size was 16 nm. Then, photocatalytic processes were started for the removal of methylene blue (MB) dye by combining the catalysis of NPs under the photocatalysis of sunlight. The degradation process provided by photocatalytic processes was carried out every half hour for 150 minutes. As a result of 150 minutes, the photodegradation efficiency was calculated to be 70%. This study supports future photodegradation studies for the removal of waste dyestuffs.

1. Introduction

Human beings are developing technology day by day. Industry is of great importance in the developing technological process [1]. Therefore, the industry is developing in parallel. This progress is developing further in various branches during the developing industrial process [2, 3]. The industrial process manifests itself in agriculture [4, 5], dyestuffs [6, 7], fertilizers [8–10], food processing processes [11, 12], and many other fields [13, 14]. Industry has many benefits as well as harm to human beings [15, 16]. For example, waste dyestuffs and waste chemicals discharged from processes mix with water and soil, causing serious harm to nature, the ecosystem, and thus the health of living things [17]. For this reason, researchers have turned to studies on the removal of waste dyestuffs and chemicals removed from the processes [18]. Among these studies, photocatalytic degradation studies have become a very remarkable field.

Photocatalysis is a process based on the removal of harmful chemical dyes by using sunlight under UV photons [19, 20]. In photocatalytic studies, photons act as a catalyst and have an effect on the breakdown and removal of dyestuffs [21]. Dyes used in photodegradation studies are generally inductors such as methylene blue (MB) [22], rhodamine B [23], or methyl orange [24]. Various reports have appeared in the literature in this field of study. For example, zinc-oxide nanoparticles were supported with activated carbon to create new nanoparticle derivatives (NPs), and the degradation of rhodamine B with UV was investigated and the efficiency was determined to be 76% [25]. In another study, zinc nanoparticles were synthesized and it was observed that the photocatalytic process was effective under UV light [26]. Photocatalytic studies using titanium oxide nanoparticles also take their place in the literature [27]. As can be seen from these exemplary reports in the literature, nanoparticles are used quite frequently in photocatalytic studies.

Nanotechnology is a branch of science that covers working sizes between 1-100 nm [28–30]. Nanotechnology, which deals with such small-sized particles, therefore enters almost every field of human science [31]. The main ones are fields such as sensors [32–36], energy studies [37–39], photocatalysis [40, 41], chemistry [42, 43], biology [44, 45], medicine [32, 46], optics [47] electronics [48, 49], etc. In photocatalytic reactions, UV light acts as a photocatalyst. Metal nanoparticles create a great synergistic effect by acting as a supporting element for photocatalysts in the photocatalytic process, and photocatalysis occurs faster, more actively, and more efficiently [50]. Bimetallic palladium-zinc nanoparticles were synthesized from *Citrus Paradisi* (grapefruit peels) and their energy activity and photocatalytic activity took place in previous studies [51]. Trimetallic palladium-platinum-cobalt nanoparticles synthesized from *Malus domestica* peels (red apple peels) also took their place in photocatalytic activity [52]. As can be understood from here, nanoparticle production from natural resources as green synthesis has a highly interesting feature.

Green synthesis is a synthesis method carried out from plant leaves [53, 54], plant roots [55, 56], plant bodies [57, 58], algae [59], fungi [60], bacteria [61], and completely natural resources in nature [58]. The advantage of green synthesis is that it does not contain chemicals and is a process that is extremely friendly to the health of living things and the ecosystem [58, 62]. In previous studies, nanoparticle production from *Nigella Sativa* seeds (black cumin seeds) has taken its place in the literature [44, 63]. Likewise, nanoparticle studies synthesized from propolis, a honey product, have also been reported [64]. In this study, synthesizing zinc nanoparticles from *Hypericum calycinum* L. leaves using the green synthesis method and carrying out the photocatalytic process attracted our attention due to their functional functions and groups, which have a feature that attracts much attention.

In this study, zinc nanoparticles (Zn NPs) were synthesized from *Hypericum calycinum* L. leaves by a biogenic method using green synthesis, and their photocatalytic activation was examined. To better observe the morphological structure of Zn NPs, photocatalytic activation efficiency was calculated by taking ultra-violet visible (UV-Vis), transmission electron microscopy (TEM), X-ray diffraction analysis (XRD) and Fourier infrared microscopy (FTIR) characterizations.

2. Material & Method

2.1. Materials

MB, Zinc (II) chloride ($ZnCl_2$), and all materials were obtained from Sigma & Aldrich. *Hypericum calycinum* L. leaves were collected from the *Yuvacik* part of *Basiskele* district of *Kocaeli.*

2.2. Instruments

Hitachi HT-7700 brand TEM device was used to elucidate the morphological structure of NPs and calculate their size. A Panalytical Empyrean brand XRD device was used to measure the crystalline size of Zn NPs. To observe the band vibrations of NPs, a Panalytical Empyrean brand device was used for

FTIR analysis. Measurement of absorbance values of plant leaves and NPs and photocatalytic studies were carried out on the HITACHI/U-4100 brand UV-Vis NIR device.

2.3. Synthesis of Zn NPs

5 g of *Hypericum calycinum* L. leaves were weighed and the extract was extracted in 100 ml of distilled water using the microwave method. Then, 25 ml of this extract was separated and 25 mg of previously weighed $ZnCl_2$ powder was added to obtain a new mixture. This resulting mixture was left at 70 ^{o}C for three days until the color change occurred [43]. After the color change occurred, the NPs were washed by filtration, dried in the oven, and stored for photocatalytic processes.

2.4. Photocatalytic studies

For photocatalytic processes, 10 mg Zn NPs were dissolved in 100 ml ultrapure water by sonicating for half an hour. Then, 1 mg MB was added and UV-Vis characterization was taken. Then, the photocatalytic efficiency was calculated by keeping this mixture in sunlight for half an hour and taking UV-Vis measurements again every half hour [52].

3. Results & Discussion

3.1. UV-Vis

UV-Vis characterization was carried out to observe the absorbance values of Zn NPs and the extract of plant leaves. Figure 1 shows the UV-Vis characterization. According to Fig. 1a, it was observed that the extract of *Hypericum calycinum* L. leaves showed two small peaks at 316 and 368 nm. In previous studies, it was observed that the *Hypericum* family also peaked in these absorbance ranges [65, 66]. According to Fig. 1b, it was observed that the absorbance of Zn NPs synthesized from *Hypericum calycinum* L. by green synthesis was very weak at 274 and 370 nm [67, 68].

3.2. FTIR

FTIR analysis was performed to observe the stretching vibrations of Zn NPs. Figure 2 shows the FTIR analysis of nanoparticles. According to Fig. 2, The distinct and sharp peak at 3252 cm^{-1} indicates the presence of Zn NPs [69]. Stretching and vibration bands indicate C-Cl, C-Cl, C-N and C-N groups originating from alkyl halides and aliphatic amines appeared at 857, 1003, and 1083 cm^{-1}, respectively [70]. Also these groups are indicating to C-O group [69]. The symmetric peak appearing at 1434 and 1616 cm^{-1} refers to nitro derivatives coming from aliphatic groups [70]. The peak seen in the 463 cm^{-1}band refers to Zn NP, which supports the reports [69], [70].

3.3. XRD

Figure 3 shows the XRD characterization analysis of Zn NPs. According to the XRD characterization, peaks appeared at 26.25°, 28.92°, 31.78°, 35.01°, 35.81°, 45.89°, 54.54°, and 62.57 theta degrees, and these peaks are (121), (111), (100), (002), (101), (102), (110) and (103) refer to lattice structures respectively [71]. According to calculations obtained from XRD characterization, the crystalline size of the nanoparticles was found to be 16 nm. This result supports previous reports with Zn NPs [69].

3.4. TEM

TEM characterization was performed to calculate the size of the synthesized Zn NPs and observe their morphological structure. TEM analysis results are given in Fig. 4. According to Fig. 4a, the image of Zn NPs taken at 100 nm scale is shown. According to Fig. 4, the nanoparticles partially agglomerated and clustered in some places, but no agglomeration was observed in some places. The size of Zn NPs was calculated as 29.066 ± 10.561 nm and the histogram is shown in Fig. 4b.

4. Results & Discussion

Photocatalytic studies were carried out in the range of 0-150 minutes, and UV-Vis analysis was performed by exposing the NP-containing with MB dye sample to the photocatalysis of sunlight every half hour (Fig. 5). In Fig. 5a, the effect of the photocatalyst every half hour is shown under UV-Vis. According to this analysis, it was observed that there was a decrease in the peak absorbance observed every half hour. In the latest application, the photodegradation efficiency was calculated to be 70% and is shown as a histogram graph in Fig. 5b.

Figure 5. Photocatalytic studies performances (a) UV–Vis graphs of MB dye in a time-bound study (b) the histogram graph of efficiency photodegradation.

Photodegradation of the photocatalyst under sunlight at 30-minute intervals occurred with the addition of MB dye. Therefore, with the addition of MB concentration, this degradation occurred and the degradation effect was further increased with each passing half hour. Figure 6 shows the graphs of photodegradation versus time with the addition of MB dye. The degradation graph of the rate formed by adding MB concentration against time is shown in Fig. 6a, and it is seen that the degradation increases with time. The graphic curve of the linear photodegradation of the addition of MB concentration and the rate of the first application is shown in Fig. 6b. According to Fig. 6b, the reaction rate is 0.95223 and it is observed that the degradation reaction is first order. The reaction linear kinetic rate was calculated according to Eq. 1 (Eq. 1). The reaction linear kinetic rate was calculated according to Eq. 1 (Eq. 1).

$In(C/C_0) = kt$ (Eq. 1) [72].

According to Eq. 1, C is the concentration of MB addition, C_0 is the original concentration of the sample before MB dye, k is the constant coefficient of the reaction, and t is the time. The previous studies of photocatalytic prosesses and this study results were given at Table 1.

Table 1
Photodegradation studies at previous reports and this study.

Entry	Photocatalyst	Method	Material dye of photodegradation	Efficieny of photodegradation	Ref
1	Pd@ZnO NPs	Biogenic method	Rhodamine B (Rh B)	75%	[73]
2	$ZnFe_2O_4$ NPs	Sol-gel/Co-precipiation/calcined at 500 ^oC method	Methyl orange (MO)	4%	[74]
3	ZnO NPs	Chemical method	Ciyanide ions (CN^-)	100%	[75]
4	W-PZn NPs	Electrochemical method	Malachite green (MG)	80%	[76]
5	Zn NPs	Biogenic method	MB	70%	**This study**

A complete scheme of oxidation reactions and how the process works through the catalyst effect of Zn NPs and the photocatalyst effect of sunlight in the photodegradation processes for MB dye removal in photocatalytic processes, from the very beginning of the process to the results, is given in Fig. 7.

5. Conclusion

In this study, Zn NPs were synthesized from the leaves of the *Hypericum calycinum* L. plant. According to the UV-Vis results taken to observe the absorbance range of the synthesized NPs, peaks were observed at 274 and 370 nm. It was observed that the plant's absorbance values were at 316 and 368 nm before NPs were synthesized. TEM characterization was performed to measure the morphological density and size of Zn NPs. According to TEM characterization, it was found to be 29.066 ± 10.561 nm. According to XRD characterization, the crystalline size of Zn NPs was calculated as 16 nm. Then, to examine the removal of MB dyestuff by sunlight photocatalyst, photocatalytic processes were started by including the catalysis of Zn NPs under UV-Vis. Photodegradation processes were repeated every half hour and were completed in 150 minutes. The efficiency was calculated to be 70% in the 150-minute period. These results yielded very important and effective results when compared to previous reports.

Declarations

Acknowledgement

We would like to thank the Ataturk University DAYTAM unit for shooting the characterizations. We would like to thank the Selcuk University ILTEK unit for the photodegradation studies. We would like to thank Onur Altinbasak and Betul Buyukkilic Altinbasak for collecting *Hypericum calycinum* L. leaves and providing plant support to our study.

Availability of data and materials All data generated or analyzed during this study are available from the corresponding author upon reason - able request.

Conflict of interest The authors declare they have no competing interests.

References

1. Drejer A, Riis JO. Competence development and technology: How learning and technology can be meaningfully integrated. Technovation 1999;19:631–44. https://doi.org/10.1016/S0166-4972(99)00064-4.
2. Roco MC, Bainbridge WS. Converging technologies for improving human performance: Integrating from the nanoscale. J Nanoparticle Res 2002;4:281–95. https://doi.org/10.1023/A:1021152023349/METRICS.
3. Maksimovic M. Greening the Future: Green Internet of Things (G-IoT) as a Key Technological Enabler of Sustainable Development. Stud Big Data 2018;30:283–313. https://doi.org/10.1007/978-3-319-60435-0_12/COVER.
4. Kamboj A, Saluja A. Phytopharmacological review of Xanthium strumarium L. (Cocklebur). Int J Green Pharm 2010;4:129–39. https://doi.org/10.4103/0973-8258.69154.
5. Karthik L KARSSV. Biological Synthesis of Nanoparticles and Their Applications - Google Kitaplar. 2019.
6. Karimi F, Demir E, Aydogdu N, Shojaei M, Taher MA, Asrami PN, et al. Advancement in electrochemical strategies for quantification of Brown HT and Carmoisine (Acid Red 14) From Azo Dyestuff class. Food Chem Toxicol 2022;165:113075. https://doi.org/10.1016/J.FCT.2022.113075.
7. Parthasarathy P, Sajjad S, Saleem J, Alherbawi M, McKay G. A Review of the Removal of Dyestuffs from Effluents onto Biochar. Sep 2022, Vol 9, Page 139 2022;9:139. https://doi.org/10.3390/SEPARATIONS9060139.
8. Rajput VD, Singh A, Minkina T, Rawat S, Mandzhieva S, Sushkova S, et al. Nano-Enabled Products: Challenges and Opportunities for Sustainable Agriculture. Plants 2021, Vol 10, Page 2727 2021;10:2727. https://doi.org/10.3390/PLANTS10122727.
9. Rana KL, Kour D, Yadav N, Yadav AN. Endophytic microbes in nanotechnology: Current development, and potential biotechnology applications. Microb Endophytes Prospect Sustain Agric 2020:231–62. https://doi.org/10.1016/B978-0-12-818734-0.00010-3.
10. Wagenfeld JG, Al-Ali K, Almheiri S, Slavens AF, Calvet N. Sustainable applications utilizing sulfur, a by-product from oil and gas industry: A state-of-the-art review. Waste Manag 2019;95:78–89. https://doi.org/10.1016/J.WASMAN.2019.06.002.
11. Bhargava N, Mor RS, Kumar K, Sharanagat VS. Advances in application of ultrasound in food processing: A review. Ultrason Sonochem 2021;70:105293. https://doi.org/10.1016/J.ULTSONCH.2020.105293.

12. Lafarga T, Fernández-Sevilla JM, González-López C, Acién-Fernández FG. Spirulina for the food and functional food industries. Food Res Int 2020;137:109356. https://doi.org/10.1016/J.FOODRES.2020.109356.
13. Maddikunta PKR, Pham QV, B P, Deepa N, Dev K, Gadekallu TR, et al. Industry 5.0: A survey on enabling technologies and potential applications. J Ind Inf Integr 2022;26:100257. https://doi.org/10.1016/J.JII.2021.100257.
14. Llopis-Albert C, Rubio F, Valero F. Impact of digital transformation on the automotive industry. Technol Forecast Soc Change 2021;162:120343. https://doi.org/10.1016/J.TECHFORE.2020.120343.
15. Vom Saal FS, Vandenberg LN. Update on the Health Effects of Bisphenol A: Overwhelming Evidence of Harm. Endocrinology 2021;162:1–25. https://doi.org/10.1210/ENDOCR/BQAA171.
16. Martin KE. Ethical issues in the big data industry. MIS Q Exec 2015;14:67–85. https://doi.org/10.4324/9780429286797-20/ETHICAL-ISSUES-BIG-DATA-INDUSTRY-KIRSTEN-MARTIN.
17. Khan WU, Ahmed S, Dhoble Y, Madhav S. A critical review of hazardous waste generation from textile industries and associated ecological impacts. J Indian Chem Soc 2023;100:100829. https://doi.org/10.1016/J.JICS.2022.100829.
18. Mishra S, Cheng L, Maiti A. The utilization of agro-biomass/byproducts for effective bio-removal of dyes from dyeing wastewater: A comprehensive review. J Environ Chem Eng 2021;9:104901. https://doi.org/10.1016/J.JECE.2020.104901.
19. Rafiq A, Ikram M, Ali S, Niaz F, Khan M, Khan Q, et al. Photocatalytic degradation of dyes using semiconductor photocatalysts to clean industrial water pollution. J Ind Eng Chem 2021;97:111–28. https://doi.org/10.1016/J.JIEC.2021.02.017.
20. Saeed M, Muneer M, Haq A ul, Akram N. Photocatalysis: an effective tool for photodegradation of dyes—a review. Environ Sci Pollut Res 2021 291 2021;29:293–311. https://doi.org/10.1007/S11356-021-16389-7.
21. Tahir H, Saad M. Using dyes to evaluate the photocatalytic activity. Interface Sci Technol 2021;32:125–224. https://doi.org/10.1016/B978-0-12-818806-4.00005-X.
22. Shakil M, Inayat U, Khalid NR, Tanveer M, Gillani SSA, Tariq NH, et al. Enhanced structural, optical, and photocatalytic activities of Cd–Co doped Zn ferrites for degrading methyl orange dye under irradiation by visible light. J Phys Chem Solids 2022;161:110419. https://doi.org/10.1016/J.JPCS.2021.110419.
23. Jamshaid M, Nazir MA, Najam T, Shah SSA, Khan HM, Rehman A ur. Facile synthesis of Yb3+-Zn2+ substituted M type hexaferrites: Structural, electric and photocatalytic properties under visible light for methylene blue removal. Chem Phys Lett 2022;805:139939. https://doi.org/10.1016/J.CPLETT.2022.139939.
24. Iwuozor KO, Ighalo JO, Emenike EC, Ogunfowora LA, Igwegbe CA. Adsorption of methyl orange: A review on adsorbent performance. Curr Res Green Sustain Chem 2021;4:100179.

https://doi.org/10.1016/J.CRGSC.2021.100179.

25. Karimi F, Altuner EE, Gulbagca F, Tiri RNE, Sen F, Javadi A, et al. Facile bio-fabrication of ZnO@AC nanoparticles from chitosan: Characterization, hydrogen generation, and photocatalytic properties. Environ Res 2023;216:114668. https://doi.org/10.1016/J.ENVRES.2022.114668.
26. Wu Y, Altuner EE, El Houda Tiri RN, Bekmezci M, Gulbagca F, Aygun A, et al. Hydrogen generation from methanolysis of sodium borohydride using waste coffee oil modified zinc oxide nanoparticles and their photocatalytic activities. Int J Hydrogen Energy 2022. https://doi.org/10.1016/J.IJHYDENE.2022.04.177.
27. Kite S V., Sathe DJ, Kadam AN, Chavan SS, Garadkar KM. Highly efficient photodegradation of 4-nitrophenol over the nano-TiO2 obtained from chemical bath deposition technique. Res Chem Intermed 2020;46:1255–82. https://doi.org/10.1007/S11164-019-04032-7/SCHEMES/2.
28. Altuner EE, Gur T, Şen F. Ternary/quaternary nanomaterials for direct alcohol fuel cells. Nanomater Direct Alcohol Fuel Cells 2021:157–72. https://doi.org/10.1016/B978-0-12-821713-9.00001-9.
29. Altuner EE, Bekmezci M, Sen F. Diffusion and Transport Studies. Handb Magn Hybrid Nanoalloys Their Nanocomposites 2022:1–18. https://doi.org/10.1007/978-3-030-34007-0_27-1.
30. Altuner EE, Arıkan K, Burhan H, Ozdemir S, Şen F. Commercial aspects of direct alcohol fuel cells. Nanomater Direct Alcohol Fuel Cells 2021:511–24. https://doi.org/10.1016/B978-0-12-821713-9.00012-3.
31. Altuner EE, Akin M, Bayat R, Bekmezci M, Burhan H, Sen F. Challenges in commercialization of carbon nanomaterial-based sensors. Carbon Nanomater Sensors Emerg Res Trends Devices Appl 2022:381–92. https://doi.org/10.1016/B978-0-323-91174-0.00020-2.
32. Karimi F, Altuner EE, Aygun A, Bayat R, Rajendran S, Sen F. Synthesis of Silver Nanoparticles by Biogenic Methods: Characterization and Development of a Sensor Sensible to Pharmaceutical Medicine Paracetamol. Top Catal 2023;1:1–9. https://doi.org/10.1007/S11244-023-01887-4/TABLES/1.
33. Alizadeh M, Asrami PN, Altuner EE, Gulbagca F, Tiri RNE, Aygun A, et al. An ultra-sensitive rifampicin electrochemical sensor based on Fe3O4 nanoparticles anchored Multiwalled Carbon nanotube modified glassy carbon electrode. Chemosphere 2022:136566. https://doi.org/10.1016/J.CHEMOSPHERE.2022.136566.
34. Altuner EE, Ozalp VC, Yilmaz MD, Sudagidan M, Aygun A, Acar EE, et al. Development of electrochemical aptasensors detecting phosphate ions on TMB substrate with epoxy-based mesoporous silica nanoparticles. Chemosphere 2022:134077. https://doi.org/10.1016/J.CHEMOSPHERE.2022.134077.
35. Diouf A, Aghoutane Y, Burhan H, Sen F, Bouchikhi B, El Bari N. Tramadol sensing in non-invasive biological fluids using a voltammetric electronic tongue and an electrochemical sensor based on biomimetic recognition. Int J Pharm 2021;593:120114. https://doi.org/10.1016/J.IJPHARM.2020.120114.

36. Arikan K, Burhan H, Bayat R, Sen F. Glucose nano biosensor with non-enzymatic excellent sensitivity prepared with nickel–cobalt nanocomposites on f-MWCNT. Chemosphere 2021:132720. https://doi.org/10.1016/J.CHEMOSPHERE.2021.132720.
37. Wu Y, Elhouda Tiri RN, Bekmezci M, Altuner EE, Aygun A, Mei C, et al. Synthesis of novel activated carbon-supported trimetallic Pt–Ru–Ni nanoparticles using wood chips as efficient catalysts for the hydrogen generation from $NaBH_4$ and enhanced photodegradation on methylene blue. Int J Hydrogen Energy 2022. https://doi.org/10.1016/J.IJHYDENE.2022.07.152.
38. Darabi R, Alown FED, Aygun A, Gu Q, Gulbagca F, Altuner EE, et al. Biogenic platinum-based bimetallic nanoparticles: Synthesis, characterization, antimicrobial activity and hydrogen evolution. Int J Hydrogen Energy 2022. https://doi.org/10.1016/J.IJHYDENE.2022.12.072.
39. Kocak Y, Aygun A, Altuner EE, Ozdemir S, Gonca S, Berikten D, et al. Eco-friendly production of platinum nanoparticles: physicochemical properties, evaluation of biological and catalytic activities. Int J Environ Sci Technol 2023:1–12. https://doi.org/10.1007/S13762-023-05232-W/FIGURES/7.
40. Lin J, Gulbagca F, Aygun A, Elhouda Tiri RN, Xia C, Van Le Q, et al. Phyto-mediated synthesis of nanoparticles and their applications on hydrogen generation on $NaBH_4$, biological activities and photodegradation on azo dyes: Development of machine learning model. Food Chem Toxicol 2022;163:112972. https://doi.org/10.1016/J.FCT.2022.112972.
41. Ameen F, Aygun A, Seyrankaya A, Elhouda Tiri RN, Gulbagca F, Kaynak İ, et al. Photocatalytic investigation of textile dyes and E. coli bacteria from wastewater using $Fe_3O_4@MnO_2$ heterojunction and investigation for hydrogen generation on $NaBH_4$ hydrolysis. Environ Res 2023;220:115231. https://doi.org/10.1016/J.ENVRES.2023.115231.
42. Ozdemir S, Turkan Z, Kilinc E, Altuner EE, Sen F. Anoxybacillus flavithermus loaded -Fe_2O_3 magnetic nanoparticles as an efficient magnetic sorbent for the preconcentrations of Cu(II) and Mn(II). Food Chem Toxicol 2022;168:113334. https://doi.org/10.1016/J.FCT.2022.113334.
43. Ni K, Wu Y, Karimi F, Gulbagca F, Seyrankaya A, Esra Altuner E, et al. Palladium based bimetallic nanocatalysts: Synthesis, characterization and hydrogen fuel production. Fuel 2023;341:127577. https://doi.org/10.1016/J.FUEL.2023.127577.
44. Aygun A, Gülbagca F, Ozer LY, Ustaoglu B, Altunoglu YC, Baloglu MC, et al. Biogenic platinum nanoparticles using black cumin seed and their potential usage as antimicrobial and anticancer agent. J Pharm Biomed Anal 2020;179:112961. https://doi.org/10.1016/J.JPBA.2019.112961.
45. Puišo J, Jonkuviene D, Mačioniene I, Šalomskiene J, Jasutiene I, Kondrotas R. Biosynthesis of silver nanoparticles using lingonberry and cranberry juices and their antimicrobial activity. Colloids Surfaces B Biointerfaces 2014;121:214–21. https://doi.org/10.1016/j.colsurfb.2014.05.001.
46. Karimi-Maleh H, Khataee A, Karimi F, Baghayeri M, Fu L, Rouhi J, et al. A green and sensitive guanine-based DNA biosensor for idarubicin anticancer monitoring in biological samples: A simple and fast strategy for control of health quality in chemotherapy procedure confirmed by docking investigation. Chemosphere 2021:132928. https://doi.org/10.1016/J.CHEMOSPHERE.2021.132928.

47. Lahmidi S, Sert Y, Şen F, Hafi M El, Ettahiri W, Gökce H, et al. Synthesis, crystal structure, Hirshfeld surface analysis, spectral characterizations and quantum computational assessments of 1-hydroxy-3-methyl-11H-pyrido[2,1-b] quinazolin-11-one. J Mol Struct 2022;1249:131592. https://doi.org/10.1016/J.MOLSTRUC.2021.131592.
48. Demirkan B, Bozkurt S, Cellat K, Arıkan K, Yılmaz M, Şavk A, et al. Palladium supported on polypyrrole/reduced graphene oxide nanoparticles for simultaneous biosensing application of ascorbic acid, dopamine, and uric acid. Sci Reports 2020 101 2020;10:1–10. https://doi.org/10.1038/s41598-020-59935-y.
49. Keyvanfard M, Karimi-Maleh H, Karimi F, Opoku F, Kiarii EM, Govender PP, et al. Electro-catalytic amplified sensor for determination of N-acetylcysteine in the presence of theophylline confirmed by experimental coupled theoretical investigation. Sci Reports 2021 111 2021;11:1–14. https://doi.org/10.1038/s41598-020-79872-0.
50. Fageria P, Gangopadhyay S, Pande S. Synthesis of ZnO/Au and ZnO/Ag nanoparticles and their photocatalytic application using UV and visible light. RSC Adv 2014;4:24962–72. https://doi.org/10.1039/C4RA03158J.
51. Altuner EE, Gulbagca F, Tiri RNE, Aygun A, Sen F. Highly efficient palladium-zinc oxide nanoparticles synthesized by biogenic methods: Characterization, hydrogen production and photocatalytic activities. Chem Eng J Adv 2023:100465. https://doi.org/10.1016/J.CEJA.2023.100465.
52. Altuner EE, El Houda Tiri RN, Aygun A, Gulbagca F, Sen F, Iranbakhsh A, et al. Hydrogen production and photocatalytic activities from NaBH4 using trimetallic biogenic PdPtCo nanoparticles: Development of machine learning model. Chem Eng Res Des 2022. https://doi.org/10.1016/J.CHERD.2022.05.021.
53. Hu W, Lee SK, Jung MJ, Heo S Il, Hur JH, Wang MH. Induction of cell cycle arrest and apoptosis by the ethyl acetate fraction of Kalopanax pictus leaves in human colon cancer cells. Bioresour Technol 2010;101:9366–72. https://doi.org/10.1016/j.biortech.2010.06.091.
54. Taha A, Aissa M Ben, Da'na E, Rossi M, Passeri D, Scaramuzzo FA, et al. Green Synthesis of an Activated Carbon-Supported Ag and ZnO Nanocomposite for Photocatalytic Degradation and Its Antibacterial Activities. Mol 2020, Vol 25, Page 1586 2020;25:1586. https://doi.org/10.3390/MOLECULES25071586.
55. Ahmad N, Sharma S, Alam MK, Singh VN, Shamsi SF, Mehta BR, et al. Rapid synthesis of silver nanoparticles using dried medicinal plant of basil. Colloids Surfaces B Biointerfaces 2010;81:81–6. https://doi.org/10.1016/j.colsurfb.2010.06.029.
56. Acidri R, Sawai Y, Sugimoto Y, Handa T, Sasagawa D, Masunaga T, et al. Phytochemical Profile and Antioxidant Capacity of Coffee Plant Organs Compared to Green and Roasted Coffee Beans. Antioxidants 2020;9:93. https://doi.org/10.3390/antiox9020093.
57. Al-Tohamy R, Ali SS, Li F, Okasha KM, Mahmoud YAG, Elsamahy T, et al. A critical review on the treatment of dye-containing wastewater: Ecotoxicological and health concerns of textile dyes and

possible remediation approaches for environmental safety. Ecotoxicol Environ Saf 2022;231:113160. https://doi.org/10.1016/J.ECOENV.2021.113160.

58. Altuner EE, Erduran V, Sen F. Green synthesized nanomaterials for bioimaging. Synth. Bionanomaterials Biomed. Appl. Micro Nano Technol., Elsevier; 2023, p. 265–86. https://doi.org/10.1016/B978-0-323-91195-5.00023-4.
59. Pugazhendhi A, Prabakar D, Jacob JM, Karuppusamy I, Saratale RG. Synthesis and characterization of silver nanoparticles using Gelidium amansii and its antimicrobial property against various pathogenic bacteria. Microb Pathog 2018;114:41–5. https://doi.org/10.1016/j.micpath.2017.11.013.
60. Manivasagan P, Venkatesan J, Senthilkumar K, Sivakumar K, Kim SK. Biosynthesis, antimicrobial and cytotoxic effect of silver nanoparticles using a novel Nocardiopsis sp. MBRC-1. Biomed Res Int 2013;2013. https://doi.org/10.1155/2013/287638.
61. Korkmaz N, Ceylan Y, Taslimi P, Karadağ A, Bülbül AS, Şen F. Biogenic nano silver: Synthesis, characterization, antibacterial, antibiofilms, and enzymatic activity. Adv Powder Technol 2020;31:2942–50. https://doi.org/10.1016/J.APT.2020.05.020.
62. Aygün A, Gülbağça F, Nas MS, Alma MH, Çalımlı MH, Ustaoglu B, et al. Biological synthesis of silver nanoparticles using Rheum ribes and evaluation of their anticarcinogenic and antimicrobial potential: A novel approach in phytonanotechnology. J Pharm Biomed Anal 2020;179:113012. https://doi.org/10.1016/J.JPBA.2019.113012.
63. Gulbagça F, Aygun A, Altuner EE, Bekmezci M, Gur T, Sen F, et al. Facile bio-fabrication of Pd-Ag bimetallic nanoparticles and its performance in catalytic and pharmaceutical applications: Hydrogen production and in-vitro antibacterial, anticancer activities, and model development. Chem Eng Res Des 2022;180:254–64. https://doi.org/10.1016/J.CHERD.2022.02.024.
64. Tiri RNE, Gulbagca F, Aygun A, Cherif A, Sen F. Biosynthesis of Ag–Pt bimetallic nanoparticles using propolis extract: Antibacterial effects and catalytic activity on NaBH4 hydrolysis. Environ Res 2022;206:112622. https://doi.org/10.1016/J.ENVRES.2021.112622.
65. Kalliantas D, Kallianta M, Kordatos K, Karagianni CS. Micro-nano particulate compositions of Hypericum perforatum L in ultra high diluted succussed solution medicinal products. Heliyon 2021;7:e06604. https://doi.org/10.1016/J.HELIYON.2021.E06604.
66. Jarzębski M, Smułek W, Baranowska HM, Masewicz Ł, Kobus-Cisowska J, Ligaj M, et al. Characterization of St. John's wort (Hypericum perforatum L.) and the impact of filtration process on bioactive extracts incorporated into carbohydrate-based hydrogels. Food Hydrocoll 2020;104:105748. https://doi.org/10.1016/J.FOODHYD.2020.105748.
67. Fakhari S, Jamzad M, Kabiri Fard H. Green synthesis of zinc oxide nanoparticles: a comparison. Green Chem Lett Rev 2019;12:19–24. https://doi.org/10.1080/17518253.2018.1547925.
68. Raad M, Abbas T, Al-Kifaie MA, Taher MR, Al-Kifaie AMA. Fabrication of Zn/ZnO Core/Shell Nanoparticles by Laser Ablation in Liquid Technique. J Kufa-Physics 2022;14:32–40. https://doi.org/10.31257/2018/JKP/2022/140105.

69. Karimi F, Altuner EE, Gulbagca F, Tiri RNE, Sen F, Javadi A, et al. Facile bio-fabrication of ZnO@AC nanoparticles from chitosan: Characterization, hydrogen generation, and photocatalytic properties. Environ Res 2023;216:114668. https://doi.org/10.1016/J.ENVRES.2022.114668.
70. Mahalakshmi S, Hema N, Vijaya PP. In Vitro Biocompatibility and Antimicrobial activities of Zinc Oxide Nanoparticles (ZnO NPs) Prepared by Chemical and Green Synthetic Route— A Comparative Study. Bionanoscience 2020;10:112–21. https://doi.org/10.1007/S12668-019-00698-W/TABLES/2.
71. Chinnathambi A, Alahmadi TA. Zinc nanoparticles green-synthesized by Alhagi maurorum leaf aqueous extract: Chemical characterization and cytotoxicity, antioxidant, and anti-osteosarcoma effects. Arab J Chem 2021;14:103083. https://doi.org/10.1016/J.ARABJC.2021.103083.
72. Altuner EE, El Houda Tiri RN, Aygun A, Gulbagca F, Sen F, Iranbakhsh A, et al. Hydrogen production and photocatalytic activities from NaBH4 using trimetallic biogenic PdPtCo nanoparticles: Development of machine learning model. Chem Eng Res Des 2022;184:180–90. https://doi.org/10.1016/J.CHERD.2022.05.021.
73. Altuner EE, Gulbagca F, Tiri RNE, Aygun A, Sen F. Highly efficient palladium-zinc oxide nanoparticles synthesized by biogenic methods: Characterization, hydrogen production and photocatalytic activities. Chem Eng J Adv 2023;14:100465. https://doi.org/10.1016/J.CEJA.2023.100465.
74. Cheng P, Deng C, Gu M, Shangguan W. Visible-light responsive zinc ferrite doped titania photocatalyst for methyl orange degradation. J Mater Sci 2007;42:9239–44. https://doi.org/10.1007/S10853-007-1902-5/FIGURES/6.
75. Bagabas A, Alshammari A, Aboud MFA, Kosslick H. Room-temperature synthesis of zinc oxide nanoparticles in different media and their application in cyanide photodegradation. Nanoscale Res Lett 2013;8:1–10. https://doi.org/10.1186/1556-276X-8-516/TABLES/5.
76. Jose A, Sunaja Devi KR, Pinheiro D, Lakshmi Narayana S. Electrochemical synthesis, photodegradation and antibacterial properties of PEG capped zinc oxide nanoparticles. J Photochem Photobiol B Biol 2018;187:25–34. https://doi.org/10.1016/J.JPHOTOBIOL.2018.07.022.

Figures

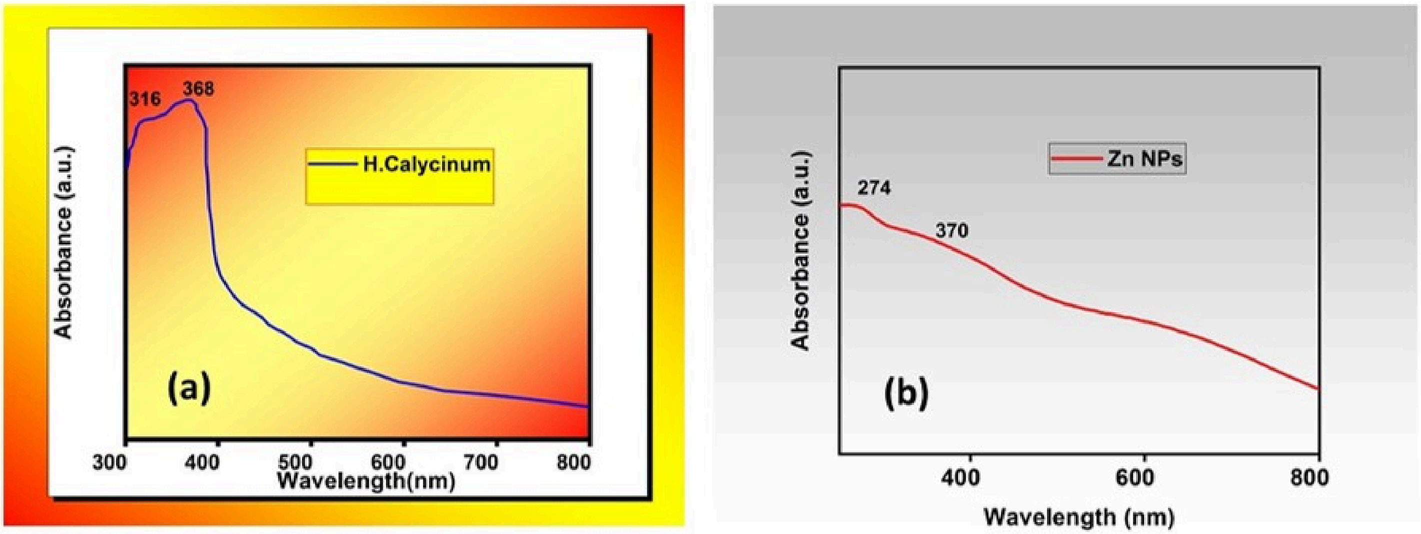

Figure 1

UV-Vis characterization of (a) *Hypericum calycinum* L. leaves and (b) Zn NPs.

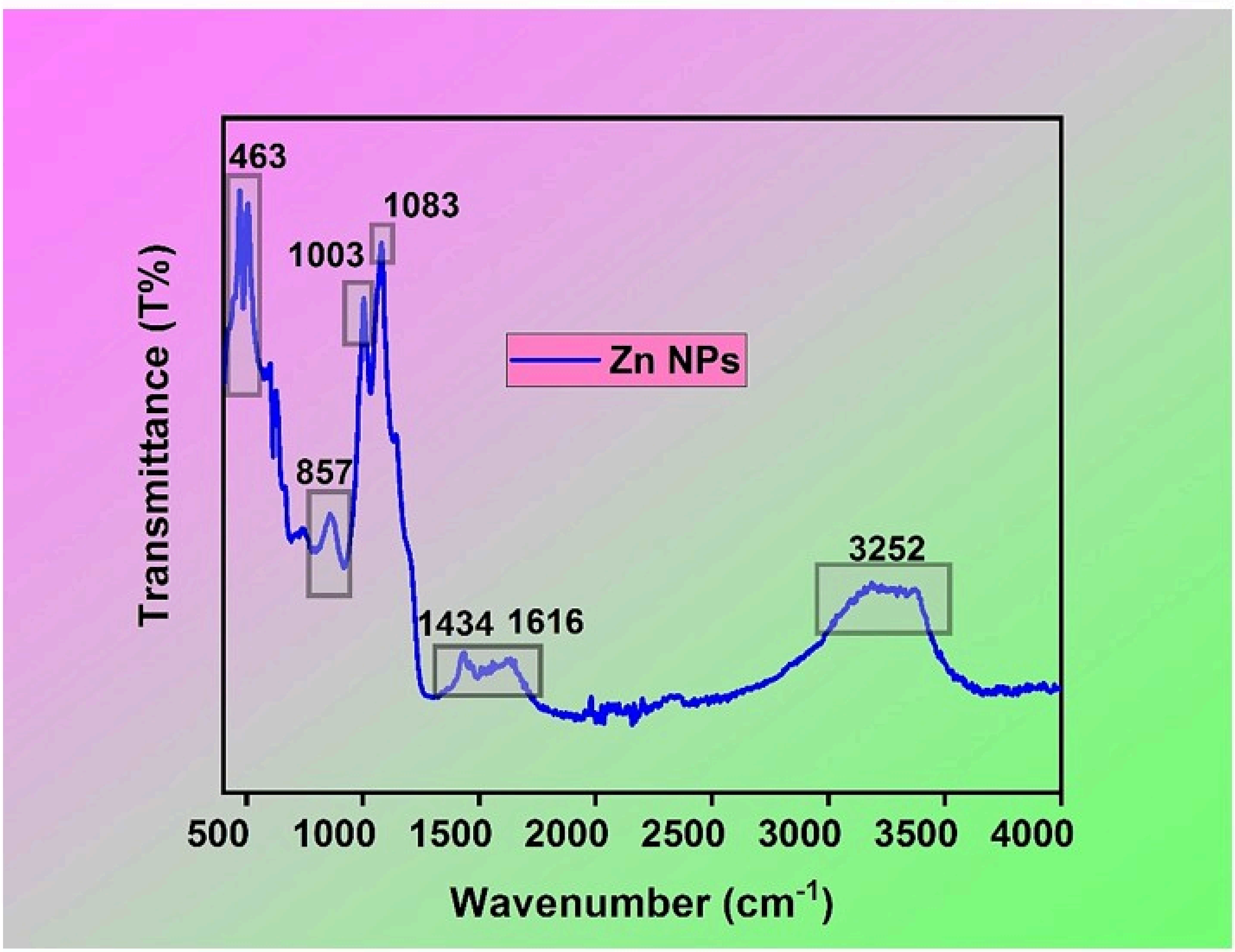

Figure 2

FTIR characterization of Zn NPs.

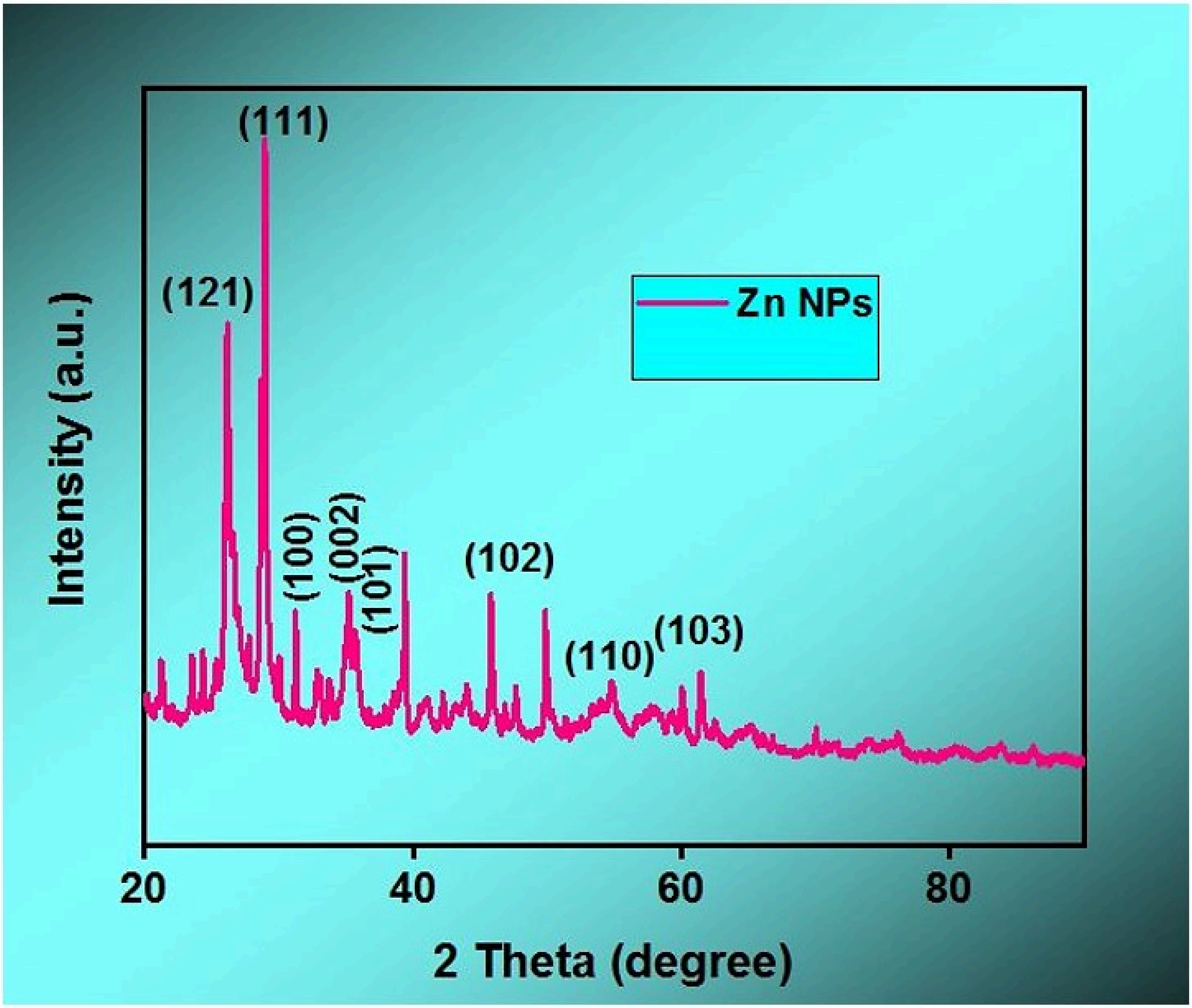

Figure 3

XRD characterization analysis of Zn NPs.

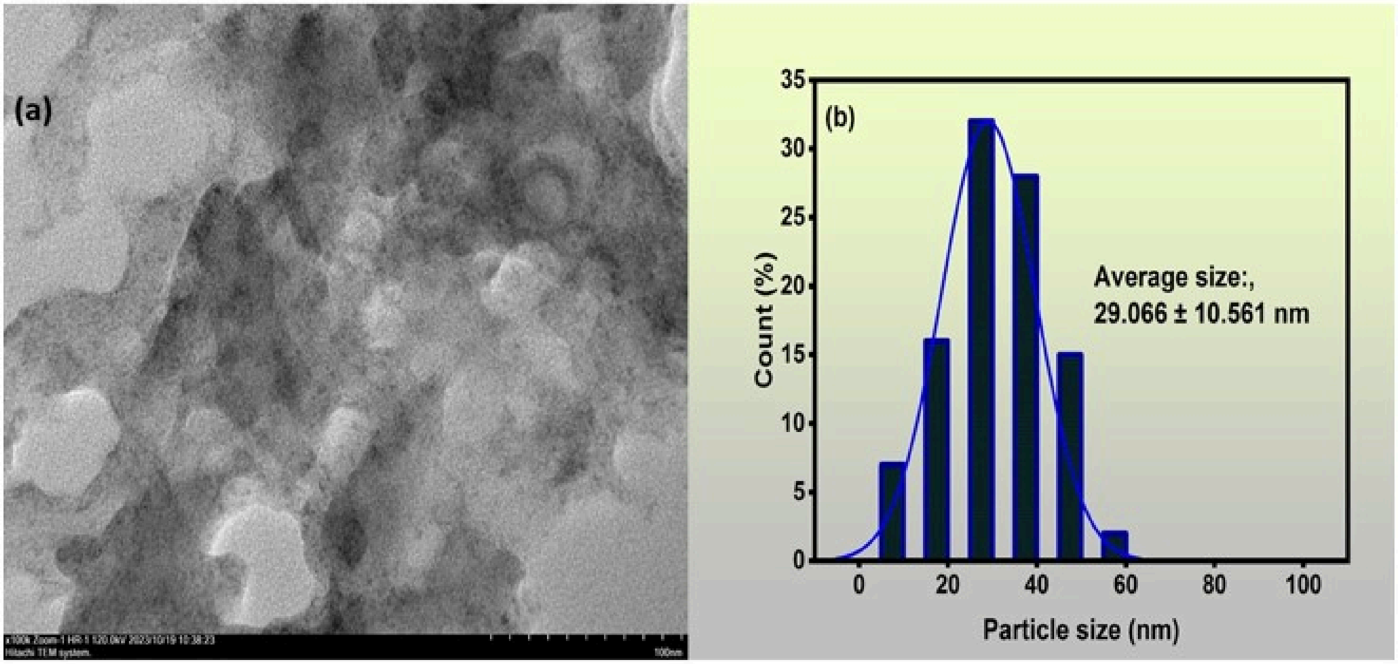

Figure 4

TEM characterization results (a) Zn NPs (b) the size histogram graph of Zn NPs.

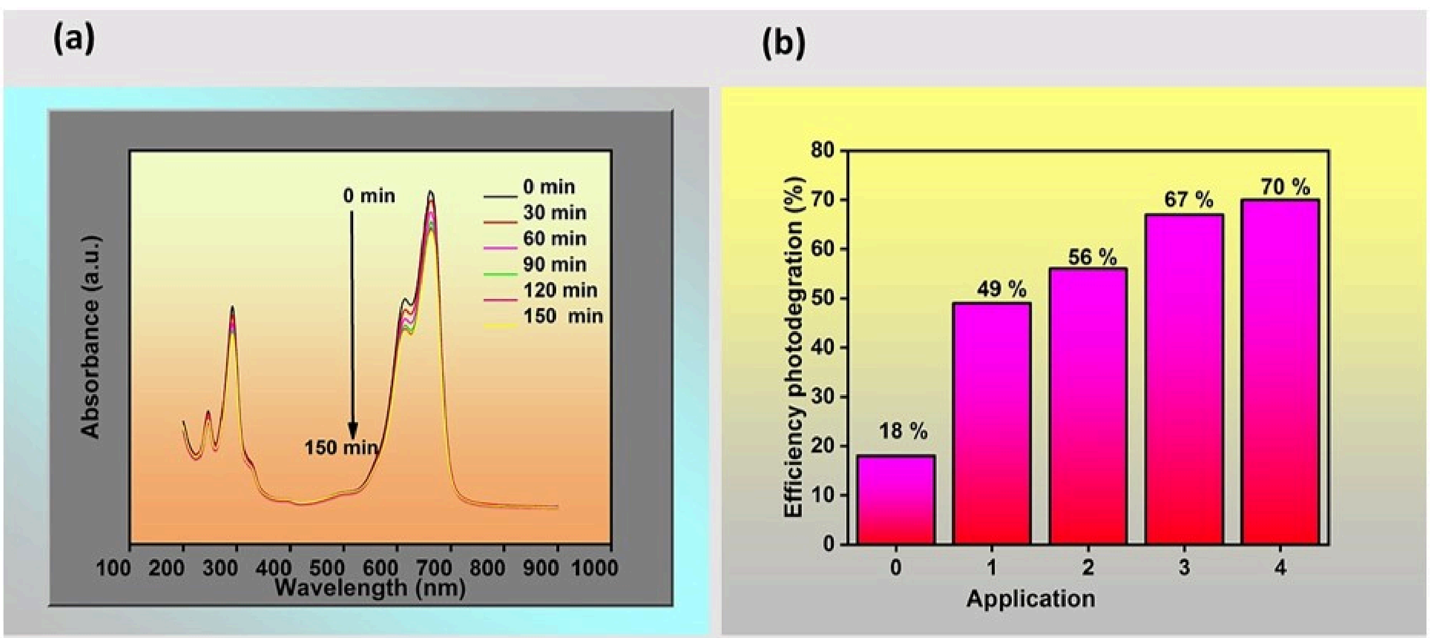

Figure 5

Photocatalytic studies performances (a) UV–Vis graphs of MB dye in a time-bound study (b) the histogram graph of efficiency photodegradation.

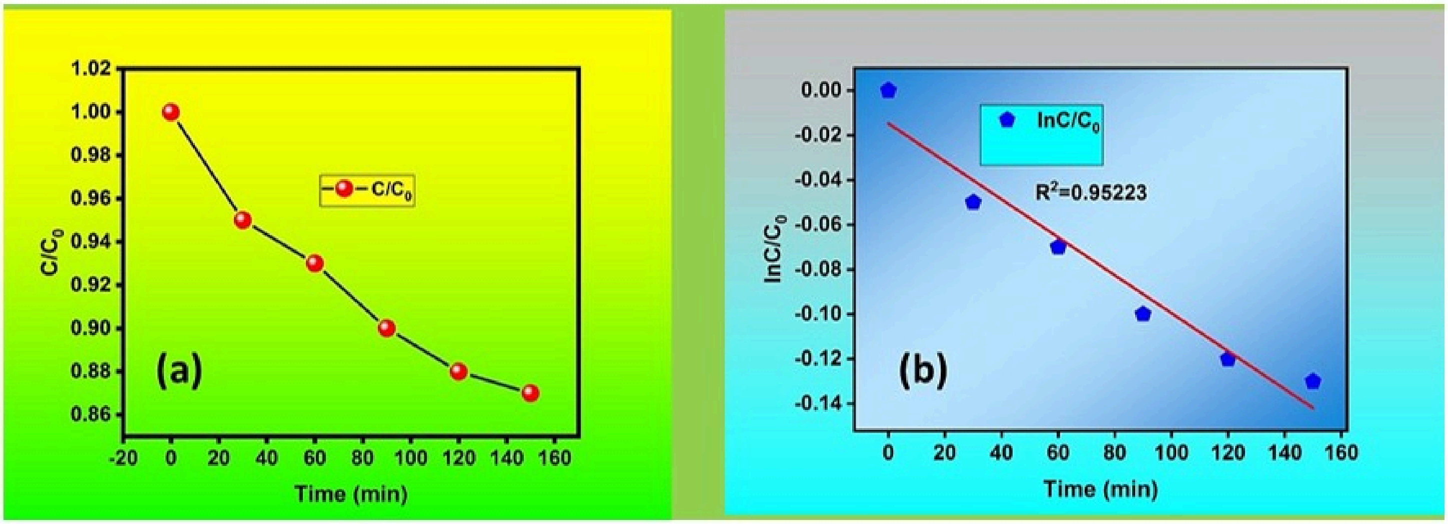

Figure 6

(a) Photodegradation curves of RhB under simulated sunlight(b) the first-order kinetics equation curves.

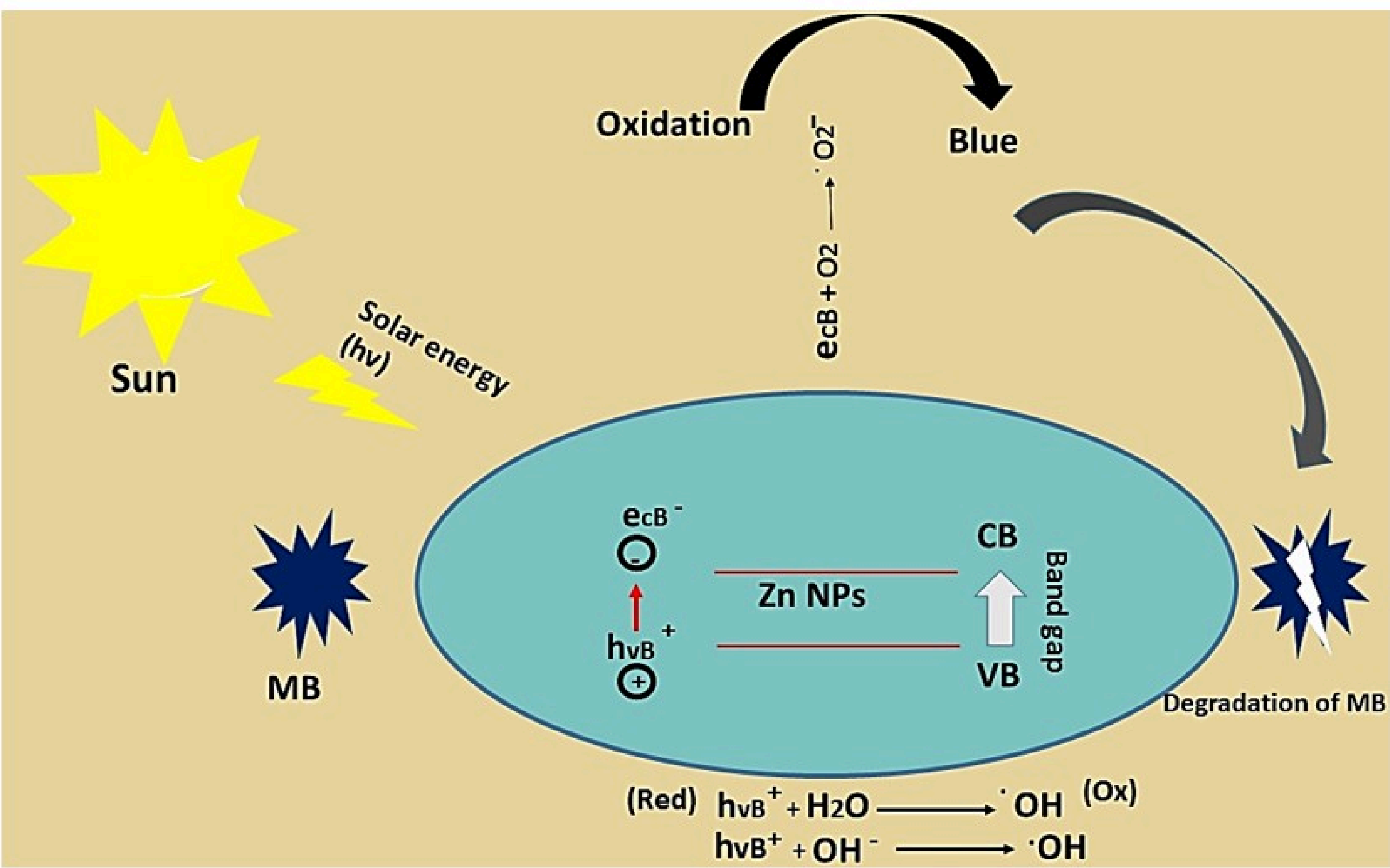

Figure 7

Illustration of MB dye using Zn NPs under photons of the sun for photocatalytic processes.

Supplementary Files

This is a list of supplementary files associated with this preprint. Click to download.

- GRAPHICALABSTRACT.docx